Molecular Microbiology (2015) 96(1), 84–94 ■
doi:10.1111/mmi.12922
First published online 30 January 2015

Pivotal and distinct role for *Plasmodium* actin capping protein alpha during blood infection of the malaria parasite

Markus Ganter,[1,2] Zaira Rizopoulos,[1] Herwig Schüler[3]* and Kai Matuschewski[1,4]*
[1]*Parasitology Unit, Max Planck Institute for Infection Biology, 10117 Berlin, Germany.*
[2]*Department of Immunology and Infectious Disease, Harvard School of Public Health, Boston, MA 02115, USA.*
[3]*Department of Medical Biochemistry and Biophysics, Karolinska Institutet, 17177 Stockholm, Sweden.*
[4]*Institute of Biology, Humboldt University, 10117 Berlin, Germany.*

Summary

Accurate regulation of microfilament dynamics is central to cell growth, motility and response to environmental stimuli. Stabilizing and depolymerizing proteins control the steady-state levels of filamentous (F-) actin. Capping protein (CP) binds to free barbed ends, thereby arresting microfilament growth and restraining elongation to remaining free barbed ends. In all CPs characterized to date, alpha and beta subunits form the active heterodimer. Here, we show in a eukaryotic parasitic cell that the two CP subunits can be functionally separated. Unlike the beta subunit, the CP alpha subunit of the apicomplexan parasite *Plasmodium* is refractory to targeted gene deletion during blood infection in the mammalian host. Combinatorial complementation of *Plasmodium berghei CP* genes with the orthologs from *Plasmodium falciparum* verified distinct activities of CP alpha and CP alpha/beta during parasite life cycle progression. Recombinant *Plasmodium* CP alpha could be produced in *Escherichia coli* in the absence of the beta subunit and the protein displayed F-actin capping activity. Thus, the functional separation of two CP subunits in a parasitic eukaryotic cell and the F-actin capping activity of CP alpha expand the repertoire of microfilament regulatory mechanisms assigned to CPs.

Accepted 5 January, 2015. *For correspondence. E-mail herwig.schuler@ki.se; Tel. +46-(0)8-524 86840; Fax +46-(08)-524 86868 or matuschewski@mpiib-berlin.mpg.de; Tel. +49-(0)30-2846 0535; Fax +49-(0)30-2846 0225. The authors declare no conflict of interest.

Introduction

Pathogenic eukaryotes of the genus *Plasmodium*, the etiological agent of malaria, rely on active motility to infect their host cells (Frénal and Soldati-Favre, 2009; Sibley, 2011; Montagna *et al.*, 2012). Progress through their life cycle is characterized by continuous stage conversion and a programmed sequence of proliferating and invasive stages (Sattler *et al.*, 2011; Montagna *et al.*, 2012). During the brief extracellular phases, parasites adopt distinct motile forms, termed merozoites, ookinetes and sporozoites. Unlike the slow, amoeboid motility displayed by other eukaryotic cells, gliding motility of *Plasmodium*, and other apicomplexan parasites, is fast (1–3 μm s^{-1}) and does not involve apparent changes in cell shape (Vanderberg, 1974; Münter *et al.*, 2009). The force that drives the parasite forward is provided by the interaction of myosins (class XIV) with filamentous (F-) actin (Dobrowolski *et al.*, 1997a; Meissner *et al.*, 2002; Morrissette and Sibley, 2002; Siden-Kiamos *et al.*, 2011). Although most *Plasmodium* actin seems to be in the monomeric, globular (G-) actin conformation (Field *et al.*, 1993; Dobrowolski *et al.*, 1997b), gliding motility apparently requires F-actin, as drug inhibition of F-actin dynamics translates into defective motility and impaired host cell invasion (Dobrowolski *et al.*, 1997a; Münter *et al.*, 2009; Hegge *et al.*, 2010).

Until recently, F-actin could not be visualized in apicomplexan parasites under physiological conditions (Gantt *et al.*, 2000; Kudryashev *et al.*, 2010). This virtual absence of F-actin in highly motile parasites is supported by consistent *in vitro* polymerization assays using recombinant and parasite-derived *Plasmodium* actin (Schmitz *et al.*, 2005; 2010; Schüler *et al.*, 2005; Sahoo *et al.*, 2006; Skillman *et al.*, 2011; 2013). These studies revealed that actin1 forms exceptionally short and unstable filaments, which could only be detected in the presence of stabilizing drugs, such as phalloidin. The recent generation of conformation-specific anti-*Plasmodium* actin1 antibodies further supported the notion of a transient actin "ring" and actin rods in invading merozoites and gliding ookinetes respectively (Riglar *et al.*, 2011; Wong *et al.*, 2011; Siden-Kiamos *et al.*, 2012). Similar short F-actin structures were identified in mutant *Toxoplasma gondii* tachyzoites, which were depleted of the G-actin-binding protein cofilin/actin depolymerizing factor (Mehta and Sibley, 2011).

Surprisingly, and in contrast to other eukaryotes, near-complete genome data sets (Gardner *et al*., 2002) suggested that the dynamics of these short actin filaments are regulated only by a minimal set of binding proteins (Baum *et al*., 2006; Schüler and Matuschewski, 2006; Sattler *et al*., 2011). Several classes of canonical actin regulators, including gelsolin, the Arp2/3 complex and WASP homology domain-containing proteins, are simply absent in *Plasmodium* genomes. One of the few conserved actin-binding proteins of *Plasmodium* parasites is the F-actin capping protein (CP), which is found in all eukaryotic organisms and metazoan cell types (Casella *et al*., 1987; Wear and Cooper, 2004; Cooper and Sept, 2008). In muscle cells, for instance, CP anchors actin filaments to the Z-disc, leading to the name CapZ (Casella *et al*., 1987; Schafer *et al*., 1993). CP binds in a calcium-independent manner to the fast-growing (barbed) ends of F-actin, thereby blocking subunit exchange (Cooper and Sept, 2008). Importantly, CP also belongs to the defined set of proteins that are needed to reconstitute actin-based motility *in vitro* (Loisel *et al*., 1999), and *CP* depletion results in reduced cell motility *in vitro* and *in vivo* (Hug *et al*., 1995; Sinnar *et al*., 2014). In addition to capping F-actin filaments, CP also stabilizes minifilaments composed of actin-related protein-1 (Arp1) (Cooper and Sept, 2008). In both cases, CP prevents addition as well as removal of actin protomers at the barbed end of the filaments. Active CP is composed of two subunits, CPα and CPβ (Cooper and Sept, 2008), and production of recombinant active CP in *Escherichia coli* is typically only achieved by co-expression of both subunits (Soeno *et al*., 1998), whereas recombinant expression of individual subunits was reported to produce insoluble protein (Remmert *et al*., 2000).

Plasmodium CPβ is encoded by a single open reading frame (Ganter *et al*., 2009), whereas *CPα* (PBANKA_124310 and PF3D7_0528500 for *Plasmodium berghei* and *Plasmodium falciparum*, respectively) is composed of nine small exons (Supporting Information Fig. S1A). Overall, *Plasmodium* CPα subunits share approximately 19% amino acid sequence identity with other eukaryotic CPα subunits, and 50–90% identity across different *Plasmodium* species (Supporting Information Fig. S1B and C). Most importantly, the residues that contribute to actin binding and heterodimer formation (Yamashita *et al*., 2003) are conserved (Supporting Information Fig. S1B).

We previously identified the CPβ subunit of the rodent malaria parasite *P. berghei* (*Pb*CPβ) as an essential regulator of sporozoite motility and malaria transmission (Ganter *et al*., 2009). Deletion of *PbCPβ* did not influence asexual and sexual blood-stage development in the mammalian host. In the insect vector, *Anopheles* mosquitoes, mutant parasites displayed defective motility, which completely arrested life cycle progression at the sporozoite stage. Our study also established that recombinant *P. berghei* CPα/β heterodimers display capping activity on heterologous non-muscle actin (Ganter *et al*., 2009). The stage-specific function of *CPβ* in sporozoites implies that *CPα* alone might be functional during blood infection of *cpβ*(–) parasites. Given that independent functions of CP subunits have not been described, this notion was unexpected and prompted us to investigate the cellular role(s) of *Plasmodium CPα* for parasite life cycle progression.

Here, we show that the CPα subunit has a distinct and important *in vivo* role during *Plasmodium* blood infection, the exclusive cause of malaria-related pathology. We also show that recombinant *Pb*CPα is stable in solution and displays actin filament capping activity in the absence of the partner β subunit.

Results

Expression profiling of Plasmodium *CP*

We first quantified *CPα* steady-state transcript levels by quantitative real-time PCR (qPCR) in three parasite stages: (i) asynchronous blood stages, (ii) schizonts and (iii) ookinetes, the stage that infects the *Anopheles* mosquito (Fig. 1A). We normalized transcript levels to *actin1* (PBANKA_145930) and compared them with the class XIV *myosin A* (*MyoA*, PBANKA_135570) and the reporter *GFP*. Although expressed in all parasite stages (Ganter *et al*., 2009), levels of both *CP* subunits were at least 30-fold lower than *MyoA* or *GFP*, in accordance with the model that only a few CP units are needed to regulate actin filaments composed of multiple actin protomers (Cooper and Sept, 2008; Sattler *et al*., 2011). We also noted a minor increase of *CPα*, but not *CPβ*, in schizonts, which is then subdivided into multiple merozoites that invade new target cells (Fig. 1A). Our qPCR data are also supported by recent RNA-seq data (Otto *et al*., 2014; Supporting Information Table S1).

Recombinant Plasmodium *CPα is stable and binds to F-actin in the absence of CPβ*

Given the results, we hypothesized that *E. coli*-expressed *Pb*CPα alone might be soluble *in vitro*. Indeed, *Pb*CPα could be readily expressed and purified as soluble protein (Fig. 1B). When we determined the approximate molecular weight by size exclusion chromatography, we observed that the ~37 kDa *Pb*CPα protein did not elute as a monomer but at an apparent molecular weight of 82 kDa. This value is consistent with a homodimer of *Pb*CPα (Fig. 1C). To confirm this result, we performed crosslinking experiments under increasing salt concentrations (Weiss *et al*., 2000). Monomers of pure recombinant CPα disappear in favor of the crosslinked putative dimer, which

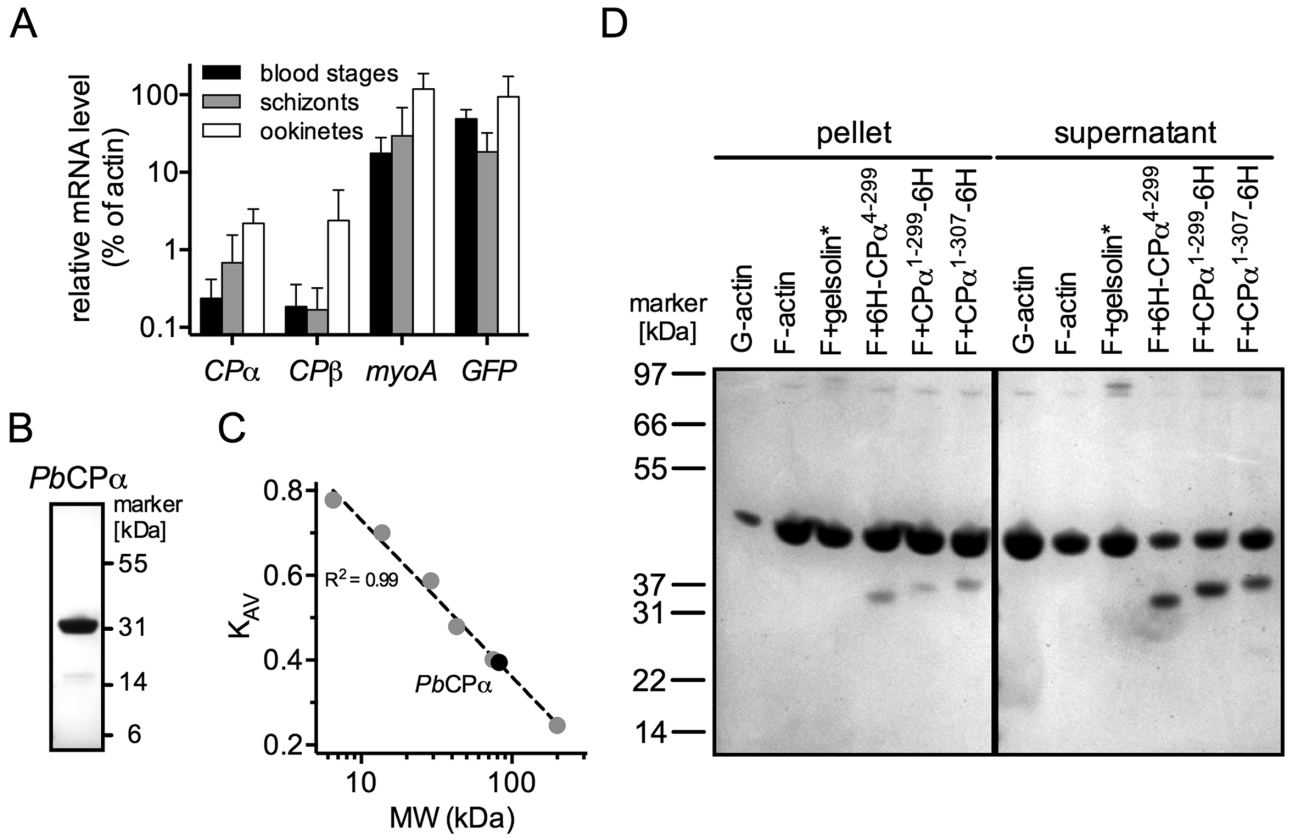

Fig. 1. *Plasmodium* CPα subunit is soluble and binds to F-actin.
A. Expression profiling of *Plasmodium berghei CPα*. Shown is a quantitative real-time PCR transcription analysis of *P. berghei CPα*, *CPβ*, *myosin A* (*myoA*) and the reporter protein *GFP* in mixed blood stages, schizonts and ookinetes. Relative mRNA levels were normalized to *actin1* transcript levels and are shown as the mean of at least two independent experiments, each done in triplicate (± standard deviation).
B. Recombinant expression and purification of soluble *Pb*CPα protein. Shown is a Coomassie-stained SDS-PAGE of recombinant purified *Pb*CPα protein.
C. Size exclusion chromatography of recombinant *Pb*CPα revealed an apparent molecular mass of ~75 kDa (black). Molecular weight standards used for this analysis are shown as gray dots.
D. *Pb*CPα specifically co-sediments with actin polymers upon ultracentrifugation. Shown is Coomassie-stained SDS-PAGE using three different recombinant purified CPα proteins. Gelsolin, denoted with an asterisk, is included as positive control.

remains even at high salt concentration (Supporting Information Fig. S2). This finding permitted us to examine the biochemical activities of recombinant *P. berghei* CPα without its cognate β subunit.

To test whether recombinant *Pb*CPα protein could interact with actin filaments, solutions of actin in the presence of three recombinant *Pb*CPα proteins were subjected to ultracentrifugation, and the pellet and supernatant fractions were analyzed by SDS-PAGE (Fig. 1D). All three proteins were recovered in the F-actin-containing pellet fraction indicative of their ability to bind to and co-sediment with F-actin. A similar analysis using varying concentrations of *Pb*CPα confirmed that presence of the protein in the pellet fraction depends on the presence of F-actin (Supporting Information Fig. S3). Canonical CPs, by interacting with the barbed end of F-actin, cause a shift of filament length distribution toward shorter polymers (Xu *et al.*, 1999). This is illustrated by a visible shift of actin from the pellet to the supernatant fraction in the presence of gelsolin (Supporting Information Fig. S2). We did not observe such an effect with *Pb*CPα, most likely because of the narrow regime of polymer lengths for which this effect can be detected by sedimentation velocity.

Recombinant Plasmodium *CPα exhibits capping activity* in vitro

As an alternative quantitative approach to test capping activity of recombinant *Pb*CPα, we employed fluorescent microscopy of actin polymers (Xu *et al.*, 1999). The presence of CPs shortens actin filaments by blocking the fast-growing (barbed) end. We determined the length distribution of fluorescently labeled actin polymers in presence or absence of recombinant *Pb*CPα (Fig. 2A). Bovine gelsolin, which not only binds to the barbed end but also severs filaments, served as control (Harris and Weeds,

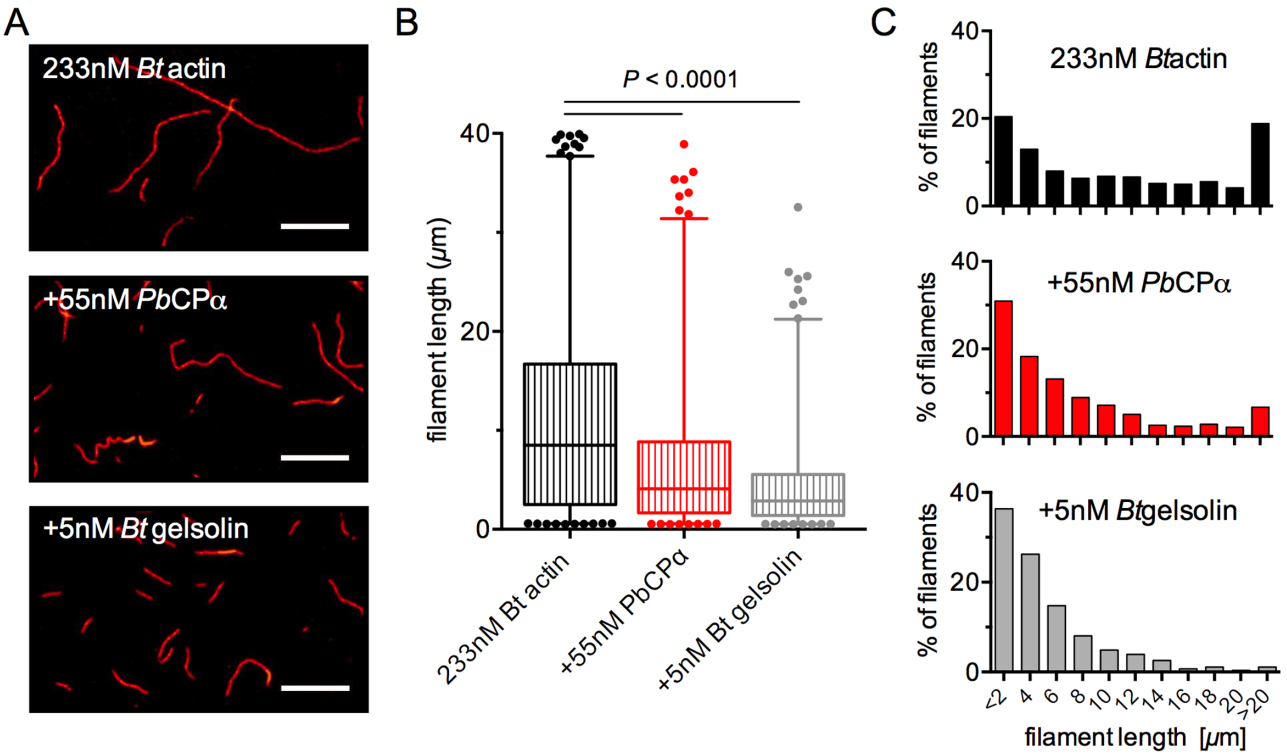

Fig. 2. *Pb*CPα exhibits capping activity *in vitro*.
A. Representative images of Alexa Fluor® 546 phalloidin-stained filaments of non-muscle bovine actin alone (*Bt* actin; upper panel), in the presence of recombinant *Plasmodium berghei* CPα (+ 55 nM *Pb*CPα; middle panel) or in the presence of bovine gelsolin (+ 5 nM *Bt* gelsolin; lower panel); bars = 10 μm.
B. Box plot of filament length distribution of bovine actin alone (*Bt* actin) or in presence of 55 nM *Pb*CPα or 5 nM bovine gelsolin respectively. The length of filaments was determined by employing ImageJ software; polymers shorter than 0.5 μm and longer than 40 μm were omitted from the analysis ($n = 1038$ for *Bt* actin, 853 for *Bt* actin + 55 nM *Pb*CPα and 820 for *Bt* actin + 5 nM *Bt* gelsolin). Boxes contain 50% of the data distributed around the median (bar); whiskers extend to the extreme observations within the 1st and 99th percentiles.
Bonferroni-corrected *P* values were determined by Mann–Whitney test.
C. Filament length distribution from B. Polymer lengths were sorted into 2 μm bins and the percental distribution plotted.

1984; Bearer, 1991; Sun *et al.*, 1994). Upon addition of recombinant *Pb*CPα to a fourfold molar excess of heterologous bovine actin, the median actin filament length significantly decreased from 8.5 μm to 4.1 μm ($P < 0.0001$). Gelsolin reduced the median filament length to 2.9 μm at a 47-fold molar excess of actin ($P < 0.0001$) (Fig. 2B).

In the presence of *Pb*CPα, the percentage of filaments between 20 and 40 μm substantially decreased (from 19% to 7%), while the percentage of filaments between 0.5 and 2 μm increased (from 20% to 31%). Upon addition of gelsolin, only 1% of filaments were 20–40 μm and 36% were 0.5–2 μm (Fig. 2C). Together, these findings show that *Pb*CPα alone displays capping activity *in vitro*.

P. berghei CPα *is refractory to targeted gene deletion*

Viability of *cpβ*(–) parasites during blood infection in mice (Ganter *et al.*, 2009) prompted us to design an experimental genetics strategy to select a similar *cpα*(–) mutant. To this end, we generated a targeting plasmid (p*CPα*REP) to replace the *P. berghei* CPα coding region with the positive selectable marker *T. gondii DHFR/TS* [Fig. 3A (i)]. In striking contrast to *CPβ* (Ganter *et al.*, 2009), we failed to generate viable recombinant *cpα*(–) parasites in three independent transfection experiments, each conducted in duplicate (Supporting Information Fig. S4). Failure to select *cpα*(–) parasites could be either due to an essential function of *Pb*CPα in asexual blood-stage parasites, the stage where transfection is performed, or refractoriness of the *PbCPα* gene locus to gene targeting.

To distinguish between these two possibilities, we generated a targeting vector for trans-species complementation of the *PbCPα* gene, employing the ortholog from the human malaria parasite *P. falciparum* (*PfCPα*) [Fig. 3A (ii)]. Upon successful transfection, *PfCPα* is expressed under the control of the endogenous *P. berghei* promoter and the heterologous *P. berghei DHFR/TS 3′* untranslated region. The first transfection of the functional *P. falciparum CPα* copy readily resulted in recombinant parasites,

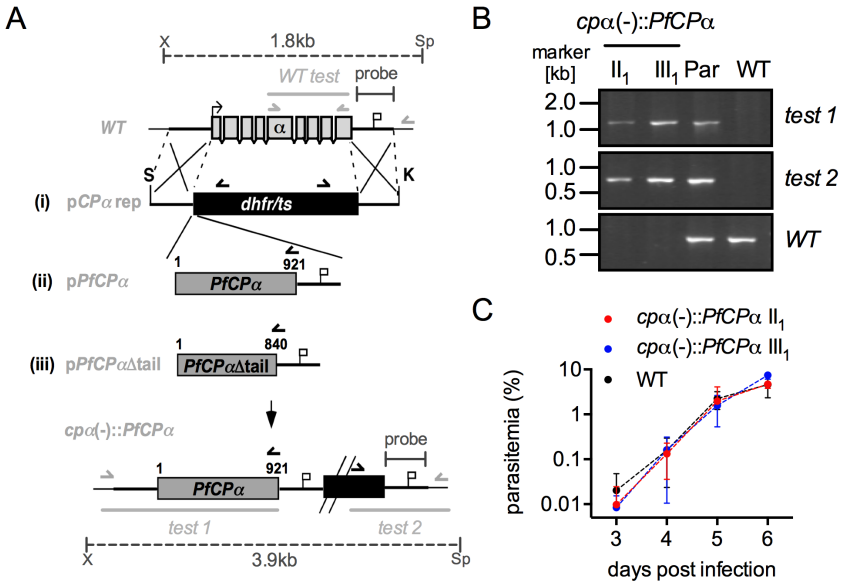

Fig. 3. *Plasmodium berghei* CPα is essential for asexual blood stages and can only be targeted in the presence of functional *Plasmodium falciparum CPα*.
A. Replacement and complementation strategies to generate the potential *cpα*(–) and transgenic *PfCPα* parasites. The *CPα* ORF is targeted with a replacement vector that either contains (i) the selection cassette only, (ii) the orthologous *P. falciparum* (*PfCPα*) gene or (iii) a truncated version lacking the C-terminal 27 amino acids (*PfCPα*Δtail). Numbers indicate the length of the transgene in base pairs. Replacement-specific test primer combinations are indicated by arrows and expected fragments are shown as lines. Capped lines indicate the probe for diagnostic Southern blot; dotted capped lines indicate the expected genomic fragments upon *Xho*I (X) and *Spe*I (Sp) digest. Constructs were linearized using *Sac*II (S) and *Kpn*I (K) respectively.
B. Genotyping of two clonal *cpα*(–)::*PfCPα* parasite lines (II_1 and III_1) obtained by *in vivo* cloning via limiting dilution. Genomic DNA from parental (par) and wild-type (WT) parasites serves as controls.
C. Asexual blood stage development of *cpα*(–)::*PfCPα* II_1 and III_1, as well as WT parasites upon intravenous injection of 1000 infected red blood cells. Shown are mean parasitemias (± standard deviation) from groups of five mice per parasite line.

termed *cpα*(–)::*PfCPα* (Supporting Information Fig. S4), indicative of an essential function of *CPα* in *Plasmodium* blood infections.

We next asked whether the carboxy (C)-terminus of CPα, an important actin-binding site in the chicken ortholog (Narita *et al.*, 2006; Takeda *et al.*, 2010), also mediates vital functions in our experimental model. Truncation of the 28 C-terminal amino acids of chicken CPα led to a 5000-fold reduction in capping affinity (Wear *et al.*, 2003). We, hence, generated a *P. falciparum CPα* replacement vector containing the corresponding C-terminal truncation (*PfCPα*Δtail) [Fig. 3A (iii)]. Two independent transfections of this targeting plasmid, each conducted in duplicate, did not result in recombinant parasites (Supporting Information Fig. S4). This result indicated that the presence of the predicted actin-binding motif is essential for CPα function *in vivo*.

Together, the experimental genetics data revealed that targeted gene deletion did not resemble the phenotype of *cpβ*(–) parasites (Ganter *et al.*, 2009). This unexpected finding is strongly suggestive of independent vital role(s) of *CPα* during *Plasmodium* blood infection, where lack of *CPβ* is phenotypically silent.

Complete rescue of blood infection defects by P. falciparum CPα

To confirm and further analyze the *P. falciparum* CPα complementation, we generated two independent clonal parasite lines, termed *cpα*(–)::*PfCPα* II_1 and III_1, by limited *in vivo* dilution. Successful replacement of the endogenous *PbCPα* by the transgenic *P. falciparum CPα* was confirmed by diagnostic PCR in both lines (Fig. 3B). We tested whether the mutant parasites were able to proliferate normally during blood infection, utilizing wild-type (WT) parasites as controls (Fig. 3C). The blood stage parasitemia of both mutant parasite lines increased over time indistinguishably from WT parasites, confirming the successful trans-species complementation of *CPα*. This result also suggests that the vital *CPα* function(s) during blood infection are apparently conserved between the murine parasite *P. berghei* and the human pathogen *P. falciparum*. Together with our biochemical characterization of *Pb*CPα and our previously reported successful generation of a *cpβ*(–) mutant parasite (Ganter *et al.*, 2009), these genetic findings indicate that the α subunit can operate independently of the β subunit.

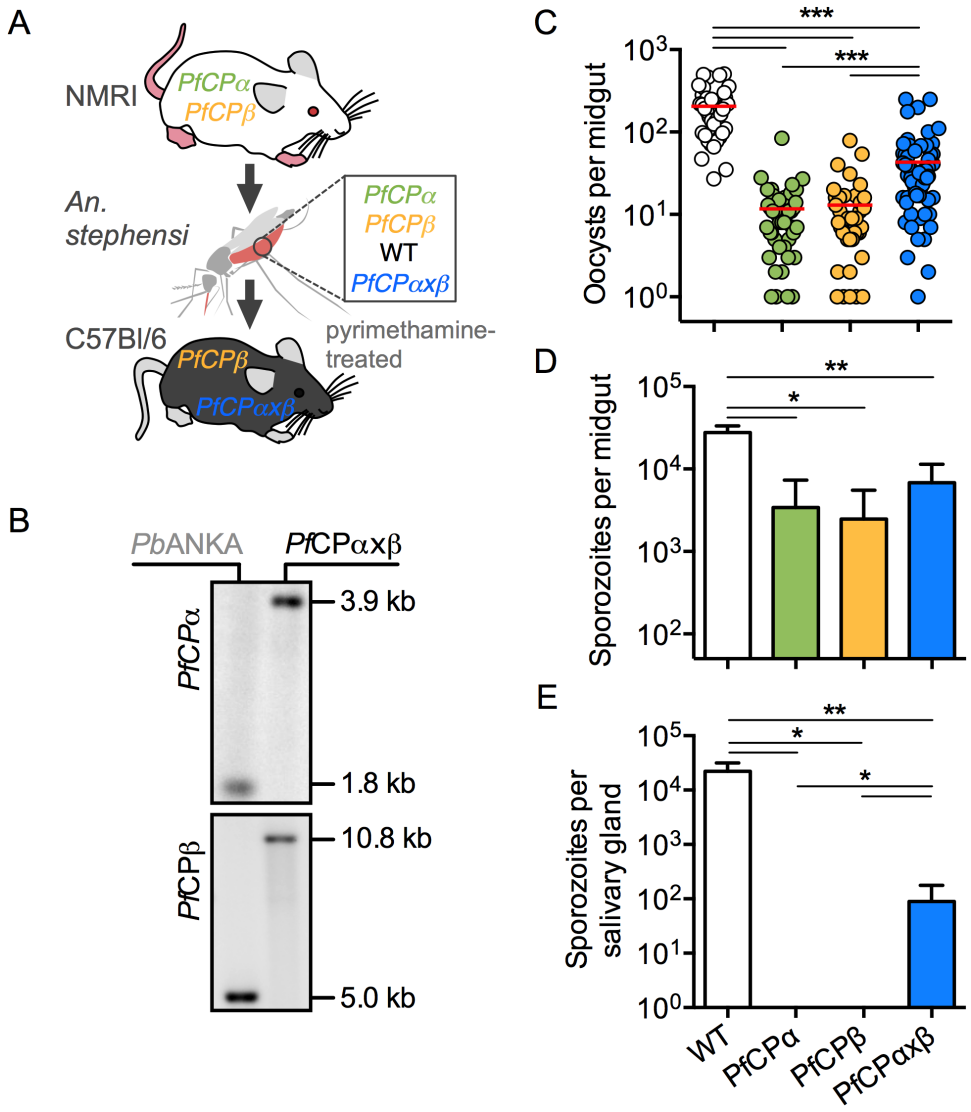

Fig. 4. *Plasmodium falciparum* CPα/CPβ complementation.
A. Scheme of the procedure to select a *cpα*(–)::*PfCPα* × *cpβ*(–)::*PfCPβ* double complemented parasite by meiotic recombination in the *Anopheles* vector and transmission to susceptible C57Bl/6 mice followed by pyrimethamine selection to counter-select for WT parasites and *in vivo* cloning to obtain a clonal parasite line. For details of sporozoite haplotypes, see Supporting Information Fig. S6A.
B. Southern blot analysis to validate the correct genotype of the selected clonal *cpα*(–)::*PfCPα*X *cpβ*(–)::*PfCPβ* double complemented parasite line.
C. Quantification of oocysts per mosquito midgut, infected with *Plasmodium berghei* WT (white), *cpα*(–)::*PfCPα* (green), *cpβ*(–)::*PfCPβ* (orange) and *cpα*(–)::*PfCPα* × *cpβ*(–)::*PfCPβ* (blue) parasites. Data are from a minimum of three independent feeding experiments. ***$P < 0.0001$ (Kruskal–Wallis test followed by Dunn's post-test).
D. Quantification of midgut-associated sporozoites on day 14 after infection. Data are from a minimum of three independent feeding experiments. *$P < 0.05$; **$P < 0.01$ (Mann–Whitney test).
E. Quantification of mature sporozoites that have colonized mosquito salivary glands on day 17 after infection. Data are from a minimum of three independent feeding experiments. *$P < 0.05$; **$P < 0.01$ (Mann–Whitney test).

Combinatorial complementation reveals distinct roles for CP subunits during Plasmodium *life cycle progression*

In marked contrast to the observed normal blood stage growth, *cpα*(–)::*PfCPα* parasites displayed defects in colonization of the *Anopheles* midgut and a complete block of salivary gland invasion (Fig. 4). Because these defects are very similar to the phenotype of *cpβ*(–) parasites (Ganter *et al.*, 2009), we generated a parasite line that harbors the *P. falciparum CPβ* in place of the endogenous *CPβ* (Supporting Information Fig. S5). Strikingly, these parasites remained defective in life cycle progression in the *Anopheles* vector as well (Fig. 4).

We hypothesized that for these stage-specific tasks, a functional CP heterodimer is necessary and that *P. berghei* and *P. falciparum* subunits are incompatible. To test this hypothesis experimentally, we generated a double complemented parasite line, *cpα*(–)::*PfCPα* × *cpβ*(–)::*PfCPβ*, by cross-fertilization and chromosomal recombination during meiosis (Fig. 4A and Supporting Information Fig. S6A). Selection of the rare recombination event, due to proximity of the two *CP* loci on chromosome XII, was augmented by counter-selection of recombined WT parasites with the antimalarial drug pyrimethamine. Natural transmission to susceptible C57Bl/6 mice and *in vivo* cloning of the resulting blood stage parasites yielded two clones, the desired *cpα*(–)::*PfCPα* × *cpβ*(–)::*PfCPβ* line and *cpβ*(–)::*PfCPβ* parasites (Fig. 4A). The latter is in good agreement with the previous finding that defective transmission of *cpβ*(–) parasites can be compensated for by presence of a WT allele during sporogony (Ganter *et al*., 2009). Southern blot analysis (Fig. 4B) and diagnostic PCR (Supporting Information Fig. S6B) confirmed successful generation of a double complemented parasite line by this strategy, already indicating that these parasites can complete the life cycle successfully.

Phenotyping of *cpα*(–)::*PfCPα* × *cpβ*(–)::*PfCPβ* parasites in the *Anopheles* vector revealed significantly more oocysts than in infections with parasites that contain single subunit complementations (Fig. 4C), indicative of partial recovery of the midgut colonization defects. Because of density dependence of oocyst-sporozoite transition (Sinden *et al*., 2007), the differences were compensated for in the production of oocyst sporozoites (Fig. 4D). Most importantly, we recovered sporozoites from salivary glands of *cpα*(–)::*PfCPα* × *cpβ*(–)::*PfCPβ*-infected *Anopheles* mosquitoes (Fig. 4E), corroborating partial recovery of the complete defect detected in infections with single subunit complementations. We interpret the finding that trans-species complementation of both subunits is needed to rescue the severe sporozoite defect as an indication that a CP heterodimer is required in mosquito stages, while CPα alone exerts vital functions during blood stage propagation.

Discussion

The most important finding of our study is that, at least in the parasitic protist *Plasmodium*, CPα exerts important functions in the absence of its cognate β subunit. This unexpected claim is supported by two complementary findings: (i) the CPα subunit of the malarial parasite has likely vital *in vivo* role(s) during asexual blood stage replication, which is not the case in *cpβ*(–) parasites, and (ii) recombinant *Pb*CPα is functional in absence of CPβ. Ablation of *CPα* is incompatible with *in vivo* proliferation of asexual blood stage parasites, whereas *CPβ* is dispensable for parasite propagation in the mammalian host (Ganter *et al*., 2009). CPα is the only remaining subunit in the latter mutant, indicating that the yet unknown vital function of *CPα* in asexual blood stages is likely performed by CPα alone, perhaps as a homodimer. Together, our reverse genetics analysis of *P. berghei* CP suggests that both subunits perform multiple, independent tasks.

We produced recombinant *P. berghei* CPα subunit, for the first time in the absence of *Pb*CPβ. The recombinant *Pb*CPα protein displayed capping activity on heterologous non-muscle actin. Inspection of the crystal structure of the chicken CPα/β heterodimer along with sequence comparison also suggests that the existence of a *Pb*CPα/α homodimer is more likely than that of a *Pb*CPα monomer (Yamashita *et al*., 2003): Taking the subunits out of their dimer context would expose the dimerization interface, creating a large unfavorable solvent-accessible hydrophobic surface. However, we cannot formally exclude the existence of monomeric pools of *Pb*CPα *in vivo*, possibly stabilized by a protein-binding partner.

When analyzing residues that make important contributions to the chicken α/β heterodimer (Yamashita *et al*., 2003), it is apparent that in most cases both bond donors and acceptors are conserved in their respective positions in *Pb*CPα (and, in fact, in *Gg*CPα). For instance, chicken CPα R259 is involved in a salt cluster with CPβ Y107, E221 and N222; all four positions are strictly conserved in the *Pb*CPα sequence (R281, Y116, E258, N259; Supporting Information Fig. S1B). This suggests the intriguing possibility of a *Pb*CPα/α homodimer that uses the same dimerization interface as the CPα/β heterodimer and a mechanism of regulation that is based on competition of available subunits, e.g. by transcriptional regulation. Based on our results, we cannot rule out *Pb*CPα homodimers with a dimer interface that differs from the one in the heterodimer; these remain important topics for future studies. Crystals of *Pb*CPα could not be produced to a quality sufficient for structure determination. Thus, the structure of *Plasmodium* CP to atomic detail remains elusive, as does the function of the 23-residue insertion. To the best of our knowledge, no evidence for CPα being active as individual subunits has been published yet, whereas a large body of literature demonstrates that CP acts as α/β heterodimers (Cooper and Sept, 2008; Pollard and Cooper, 2009).

CP stabilizes actin filaments, as well as Arp1 minifilaments, by preventing both gain and loss of monomers at the filament barbed end (Cooper and Sept, 2008; Pollard and Cooper, 2009). For this capping activity, the C-terminal tails of each subunit are crucial (Narita *et al*., 2006; Narita and Maéda, 2007). Basic residues of the CPα C-terminus initially interact with acidic amino acids of the penultimate and terminal actin protomers; the mobile CPβ C-terminus then occupies a hydrophobic pocket on

the terminal protomer (Narita *et al*., 2006; Takeda *et al*., 2010). This two-step binding model assigns a central role to the CPα C-terminus, and deletion of CPα tail led to a 5000-fold decrease in capping affinity, in contrast to a 300-fold reduction upon deletion of the CPβ C-terminus (Wear *et al*., 2003). We note that recombinant *Pb*CPα protein lacking the eight most C-terminal residues had actin capping activity and co-sedimented with actin polymers in ultracentrifugation experiments. There are several possible explanations for this. This function may not be conserved in the C-terminus of the parasite CP protein or may not come to bearing in the interaction with heterologous actin. These explanations would also be consistent with the high concentrations of *Pb*CPα, as compared with chicken CP (Wear *et al*., 2003), needed to detect an effect. Alternatively, experiments at higher resolution might be required to detect a similar effect of the *Pb*CPα C-terminal extension.

Capping activity appears to be essential throughout the *Plasmodium* life cycle. Intriguingly, in apicomplexan parasites, the two CP subunits apparently split the task of F-actin and/or Arp1 minifilament capping, as the parasite changes its cellular environment. One possible explanation is that the CPα/β heterodimer largely mediates microfilament capping at ambient temperatures in the mosquito vector, whereas the α homodimer might have evolved for the corresponding activity in the warm-blooded mammalian host. Alternatively, considering the divergent functional properties of parasite actin, F-actin and Arp1 minifilament capping may be divided between the α and β subunits. In such a scenario, the fast-moving sporozoites might rely on F-actin capping by CPα/β, while an intracellular lifestyle and host cell manipulation in general might require efficient vesicle uptake that involves the dynactin complex together with a CPα-capped Arp1 minifilament.

Birds and mammals express at least three isoforms of CPα and two isoforms of CPβ, and all display tissue-specific expression patterns (Barron-Casella *et al*., 1995; Hart *et al*., 1997; Hart and Cooper, 1999). Similarly, we identified *PbCPβ* initially as a gene that is up-regulated during sporozoite maturation (Matuschewski *et al*., 2002). While we present the first description of separate cellular roles for CP subunits, differential and tissue-specific heterodimers as a result of functional requirements appear to be established in other organisms as well. For instance, in mouse muscle cells, the two CPβ isoforms perform distinct *in vivo* functions that cannot be compensated for by the other isoform (Hart and Cooper, 1999). Together with our findings, this warrants future studies to test whether CP subunits alone exert specific functions in other eukaryotes, as seen in *Plasmodium* with its morphologically and phenotypically distinct life cycle stages.

Experimental procedures

Experimental animals

Naval Medical Research Institute (NMRI) mice were purchased from Charles River Laboratories, Sulzfeld, Germany. All animal work was conducted in accordance with the German "Tierschutzgesetz in der Fassung vom 18. Mai 2006 (BGBl. I S. 1207)", which implements directive 86/609/EEC from the European Union and the European Convention for the Protection of Vertebrate Animals used for experimental and other scientific purposes. The protocol was approved by the state authorities (LAGeSo Reg# G0469/09).

Reverse transcription and qPCR

Total RNA was purified employing the RNeasy kit (Qiagen), and reverse transcription was performed using the RETROscript kit (Ambion). qPCR was performed on cDNA preparations from mixed blood stages, purified late schizonts/merozoites and purified ookinetes using the ABI 7500 sequence detection system or StepOnePlus™ and Power SYBR® Gene PCR Master Mix (Applied Biosystems), according to the manufacturer's instructions. qPCR was performed in triplicates, with 1 cycle of 95°C for 15 min, followed by 40 cycles of 95°C for 15 s, 55°C for 15 s and 60°C for 45 s. Data were analyzed with the SDS1.3.1 software (Applied Biosystems). Relative transcript abundance was normalized to the expression of actin. The following primers were used for qPCR: *CPα*_for and *CPα*_rev; *CPβ*_for and *CPβ*_rev; *MyoA*_for and *MyoA*_rev; *actin1*_for and *actin1*_rev; and *GFP*_for and *GFP*_rev. Primer sequences are listed in Supporting Information Table S1.

Recombinant expression and purification of CPα

DNA encoding the *CPα* fragments *Pb*CPα$^{4–307}$ (L4-V307), *Pb*CPα$^{4–299}$ (L4-D299) and *Pb*CPα$^{4–292}$ (L4-Y292) were subcloned into pNIC-Bsa4 to add an N-terminal cleavable hexa-histidine tag. All proteins were expressed in *E. coli* BL21-CodonPlus cells (Stratagene) and purified using immobilized nickel ion affinity chromatography, followed by size exclusion chromatography in 20 mM HEPES (pH 7.5), 300 mM NaCl, 10% glycerol and 1 mM TCEP. The three highly similar purified proteins were used for biochemical assays as follows: *Pb*CPα$^{4–307}$ for cosedimentation with actin polymers (Supporting Information Fig. S3); *Pb*CPα$^{4–299}$ to represent expression of soluble protein (Fig. 1B), for cosedimentation with actin polymers (Fig. 1D), for capping activity of fluorescently labeled actin polymers (Fig. 2) and for the crosslinking assay (Supporting Information Fig. S2); and *Pb*CPα$^{4–292}$ for size exclusion chromatography (Fig. 1C). Two additional proteins con-

taining a C-terminal hexa-histidine tag, *Pb*CPα$^{1–307}$ (M1-V307) and *Pb*CPα$^{1–299}$ (M1-D299), were included in the cosedimentation with actin polymers (Fig. 1D). All recombinant protein batches were verified using time-of-flight mass spectrometry analysis (data not shown).

Apparent molecular mass determination

Analytical size exclusion chromatography was carried out using a 16/10 Superdex-200 column attached to an Äkta Explorer FPLC system (GE Healthcare) and buffer containing 20 mM HEPES (pH 7.5), 300 mM NaCl, 10% glycerol and 1 mM TCEP. The column was calibrated using molecular mass standards, i.e. aprotinin, ribonuclease A, carbonic anhydrase, ovalbumin and conalbumin (GE Healthcare); as well as adenosylhomocysteinase-3 log(MW) was plotted against $K_{AV} = (V_0\text{-}V_t)/(V_0\text{-}V_e)$ for each protein, where V_0 is the total column volume, V_e is the exclusion volume and V_t is the elution volume of each protein. The apparent molecular mass of *Pb*CPα was calculated from its elution volume and the regression line of the above plot.

Actin assays

The ultracentrifugation assay was conducted as previously described (Schüler and Peti, 2007) using 4 μM non-muscle bovine β-actin, *Pb*CPα and 200 nM bovine gelsolin (Sigma-Aldrich G8032). The microscopic analysis of capping activity of recombinant *Pb*CPα was carried out as described (Xu *et al*., 1999). In brief, β-actin in F-actin buffer (20 mM Tris pH 7.5, 1 mM $MgCl_2$, 100 mM KCl, 1 mM TCEP, 0.1 mM $CaCl_2$, 0.5 mM ATP, 0.1 mg ml^{-1} BSA) was incubated at room temperature for 2–3 h in the presence of 175 nM Alexa Fluor® 546 phalloidin (Invitrogen). Prior to microscopy, phalloidin-stained F-actin was diluted 1:4 in F-actin buffer either without additional protein or with 55 nM *Pb*CPα or 5 nM bovine gelsolin. Of these solutions, 3 μl was transferred onto 12 mm diameter poly-L-lysine-coated cover slips and subsequently imaged. To minimize filament severing due to shear forces, we used trimmed pipette tips at all times. Filaments were imaged on a Leica TCS SP-1 confocal microscope, and their length was determined using ImageJ software (U. S. Natl. Institutes of Health).

Parasite transfection and genotypic analysis

For targeted disruption of *PbCPα*, two fragments were amplified from *P. berghei* genomic DNA as template using primers *PbCPα*_forI and *PbCPα*_revII to amplify the 5′ flanking region, and *PbCPα*_forIII and *PbCPα*_revIV for amplification of the 3′ flanking region. Cloning into the *P. berghei* transfection plasmid b3D.DT^H.^D (Janse *et al*., 2006) resulted in the plasmid p*Pb*CPαrep. The targeting plasmid was linearized with *Sac*II and *Kpn*I; parasite transfection, positive selection and parasite cloning were then performed as previously described (Janse *et al*., 2006). Integration-specific PCR amplification of the predicted *cpα*(–) locus was done using specific primer combinations: *CPα*_5′_test_for and b3D_revX, as well as b3D Tg_rev_Pro and *CPα*_3′ test_rev. Primer sequences are listed in Supporting Information Table S2.

Single complementations of cpα*(–) and* cpβ*(–)*

In order to complement *cpα*(–) parasites, we amplified the orthologous *P. falciparum CPα* gene using the primers *PfCPα*_compforV and *PfCPα*_comprevVI and *P. falciparum* cDNA as template (Supporting Information Table S2). Cloning into the plasmid p*PbCPα*rep resulted in the complementation plasmid p*PfCPα*. For complementation with a C-terminally deleted *P. falciparum CPα* gene that lacks the last 27 amino acid residues, primers *PfCPα*_compforV and *PfCPα*_comprevVII were used, resulting in the complementation plasmid p*PfCPα*Δtail. Transfection and genotyping were conducted as described above; parasites were cloned by limiting dilution and intravenous injection of a single parasite per naïve NMRI mouse in a total of 10 animals.

To complement *cpβ*(–) parasites, we amplified the orthologous *P. falciparum CPβ* gene (PF3D7_0517600) using the primers *PfCPβ*_compforV and *PfCPβ*_comprevVI and *P. falciparum* genomic DNA as template (Supporting Information Table S2). Cloning into the plasmid p*PbCPβREP* (Ganter *et al*., 2009) resulted in the plasmid p*PfCPβ* with *PfCPβ* under the control of the endogenous *PbCPβ* promoter and the 3′ untranslated region of *Pb*DHFR/TS. Transfection and genotyping were conducted as described above; parasites were cloned by limiting dilution and intravenous injection of a single parasite per naïve NMRI mouse in a total of 10 animals. *cpβ*(–)::*PfCPβ* clones were genotyped by diagnostic PCR using primers *CPβ*_5′_test_for and *PfCPβ*_comprevVII as well as b3D Tg_rev_Pro and *CPα*_3′ test_rev (Supporting Information Table S2).

Double complementation of cpα*(–) and* cpβ*(–)*

cpα(–)::*PfCPα* × *cpβ*(–)::*PfCPβ* double complemented parasites were obtained by genetic cross of *cpα*(–)::*PfCPα* and *cpβ*(–)::*PfCPβ* clones. We fed clonal single complemented parasites to *Anopheles stephensi* mosquitoes. Upon sexual recombination and crossover, we expected to obtain a fraction of sporozoites with the desired double complementation. C57Bl/6 mice were infected by natural transmission and a clonal *cpα*(–)::*PfCPα* × *cpβ*(–)::*PfCPβ* double complemented line was isolated by limiting dilution. The genotype was confirmed by Southern blot as previously described (Ganter *et al*., 2009).

Acknowledgements

We thank Dr. Julia Sattler for the gift of bovine non-muscle actin and Klaus Rogge and Clarissa Valim, Sc.D., M.D. for assistance with the fluorescence microscopy data analysis. This work was supported by the Max Planck Society, the European Commission (EviMalaR, #34) and the Chica and Heinz Schaller Foundation to K.M., and by the Deutsche Forschungsgemeinschaft (Schwerpunktprogramm 1150) and the Structural Genomics Consortium to H.S.

References

Barron-Casella, E.A., Torres, M.A., Scherer, S.W., Heng, H.H., Tsui, L.C., and Casella, J.F. (1995) Sequence analysis and chromosomal localization of human Cap Z. Conserved residues within the actin-binding domain may link Cap Z to gelsolin/severin and profilin protein families. *J Biol Chem* **270:** 21472–21479.

Baum, J., Papenfuss, A.T., Baum, B., Speed, T.P., and Cowman, A.F. (2006) Regulation of apicomplexan actin-based motility. *Nat Rev Microbiol* **4:** 621–628.

Bearer, E.L. (1991) Direct observation of actin filament severing by gelsolin and binding by gCap39 and CapZ. *J Cell Biol* **115:** 1629–1638.

Casella, J.F., Craig, S.W., Maack, D.J., and Brown, A.E. (1987) Cap Z(36/32), a barbed end actin-capping protein, is a component of the Z-line of skeletal muscle. *J Cell Biol* **105:** 371–379.

Cooper, J.A., and Sept, D. (2008) New insights into mechanism and regulation of actin capping protein. *Int Rev Cell Mol Biol* **267:** 183–206.

Dobrowolski, J., Carruthers, V., and Sibley, L.D. (1997a) Participation of myosin in gliding motility and host cell invasion by *Toxoplasma gondii*. *Mol Microbiol* **26:** 163–173.

Dobrowolski, J.M., Niesman, I.R., and Sibley, L.D. (1997b) Actin in the parasite *Toxoplasma gondii* is encoded by a single copy gene, ACT1 and exists primarily in a globular form. *Cell Motil Cytoskeleton* **37:** 253–262.

Field, S., PInder, J., Clough, B., Dluzewski, A., Wilson, R., and Gratzer, W. (1993) Actin in the merozoite of the malaria parasite, *Plasmodium falciparum*. *Cell Motil Cytoskeleton* **25:** 43–48.

Frénal, K., and Soldati-Favre, D. (2009) Role of the parasite and host cytoskeleton in apicomplexa parasitism. *Cell Host Microbe* **5:** 602–611.

Ganter, M., Schüler, H., and Matuschewski, K. (2009) Vital role for the *Plasmodium* actin capping protein (CP) beta-subunit in motility of malaria sporozoites. *Mol Microbiol* **74:** 1356–1367.

Gantt, S., Persson, C., Rose, K., Birkett, A.J., Abagyan, R., and Nussenzweig, V. (2000) Antibodies against thrombospondin-related anonymous protein do not inhibit *Plasmodium* sporozoite infectivity in vivo. *Infect Immun* **68:** 3667–3673.

Gardner, M.J., Hall, N., Fung, E., White, O., Berriman, M., Hyman, R.W., *et al*. (2002) Genome sequence of the human malaria parasite *Plasmodium falciparum*. *Nature* **419:** 498–511.

Harris, H.E., and Weeds, A.G. (1984) Plasma gelsolin caps and severs actin filaments. *FEBS Lett* **177:** 184–188.

Hart, M.C., and Cooper, J.A. (1999) Vertebrate isoforms of actin capping protein beta have distinct functions *in vivo*. *J Cell Biol* **147:** 1287–1298.

Hart, M.C., Korshunova, Y.O., and Cooper, J.A. (1997) Vertebrates have conserved capping protein alpha isoforms with specific expression patterns. *Cell Motil Cytoskeleton* **38:** 120–132.

Hegge, S., Münter, S., Steinbüchel, M., Heiss, K., Engel, U., Matuschewski, K., and Frischknecht, F. (2010) Multistep adhesion of *Plasmodium* sporozoites. *FASEB J* **24:** 2222–2234.

Hug, C., Jay, P.Y., Reddy, I., McNally, J.G., Bridgman, P.C., Elson, E.L., and Cooper, J.A. (1995) Capping protein levels influence actin assembly and cell motility in *Dictyostelium*. *Cell* **81:** 591–600.

Janse, C.J., Franke-Fayard, B., Mair, G.R., Ramesar, J., Thiel, C., Engelmann, S., *et al*. (2006) High efficiency transfection of *Plasmodium berghei* facilitates novel selection procedures. *Mol Biochem Parasitol* **145:** 60–70.

Kudryashev, M., Lepper, S., Baumeister, W., Cyrklaff, M., and Frischknecht, F. (2010) Geometric constrains for detecting short actin filaments by cryogenic electron tomography. *PMC Biophys* **3:** 6.

Loisel, T.P., Boujemaa, R., Pantaloni, D., and Carlier, M.F. (1999) Reconstitution of actin-based motility of *Listeria* and *Shigella* using pure proteins. *Nature* **401:** 613–616.

Matuschewski, K., Ross, J., Brown, S.M., Kaiser, K., Nussenzweig, V., and Kappe, S.H.I. (2002) Infectivity-associated changes in the transcriptional repertoire of the malaria parasite sporozoite stage. *J Biol Chem* **277:** 41948–41953.

Mehta, S., and Sibley, L.D. (2011) Actin depolymerizing factor controls actin turnover and gliding motility in *Toxoplasma gondii*. *Mol Biol Cell* **22:** 1290–1299.

Meissner, M., Schlüter, D., and Soldati, D. (2002) Role of *Toxoplasma gondii* myosin A in powering parasite gliding and host cell invasion. *Science* **298:** 837–840.

Montagna, G.N., Matuschewski, K., and Buscaglia, C.A. (2012) Plasmodium sporozoite motility: an update. *Front Biosci (Landmark Ed)* **17:** 726–744.

Morrissette, N.S., and Sibley, L.D. (2002) Cytoskeleton of apicomplexan parasites. *Microbiol Mol Biol Rev* **66:** 21–38.

Münter, S., Sabass, B., Selhuber-Unkel, C., Kudryashev, M., Hegge, S., Engel, U., *et al*. (2009) *Plasmodium* sporozoite motility is modulated by the turnover of discrete adhesion sites. *Cell Host Microbe* **6:** 551–562.

Narita, A., and Maéda, Y. (2007) Molecular determination by electron microscopy of the actin filament end structure. *J Mol Biol* **365:** 480–501.

Narita, A., Takeda, S., Yamashita, A., and Maéda, Y. (2006) Structural basis of actin filament capping at the barbed-end: a cryo-electron microscopy study. *EMBO J* **25:** 5626–5633.

Otto, T.D., Böhme, U., Jackson, A.P., Hunt, M., Franke-Fayard, B., Hoejimakers, W.A.M., *et al*. (2014) A comprehensive evaluation of rodent malaria parasite genomes and gene expression. *BMC Biol* **12:** 86.

Pollard, T.D., and Cooper, J.A. (2009) Actin, a central player in cell shape and movement. *Science* **326:** 1208–1212.

Remmert, K., Vullhorst, D., and Hinssen, H. (2000) *In vitro* refolding of heterodimeric CapZ expressed in *E. coli* as inclusion body protein. *Protein Expr Purif* **18:** 11–19.

Riglar, D.T., Richard, D., Wilson, D.W., Boyle, M.J., Dekiwadia, C., Turnbull, L., *et al.* (2011) Super-resolution dissection of coordinated events during malaria parasite invasion of the human erythrocyte. *Cell Host Microbe* **9:** 9–20.

Sahoo, N., Beatty, W., Heuser, J., Sept, D., and Sibley, L.D. (2006) Unusual kinetic and structural properties control rapid assembly and turnover of actin in the parasite *Toxoplasma gondii*. *Mol Biol Cell* **17:** 895–906.

Sattler, J.M., Ganter, M., Hliscs, M., Matuschewski, K., and Schüler, H. (2011) Actin regulation in the malaria parasite. *Eur J Cell Biol* **90:** 966–971.

Schafer, D.A., Waddle, J.A., and Cooper, J.A. (1993) Localization of CapZ during myofibrillogenesis in cultured chicken muscle. *Cell Motil Cytoskeleton* **25:** 317–335.

Schmitz, S., Grainger, M., Howell, S., Calder, L.J., Gaeb, M., Pinder, J.C., *et al.* (2005) Malaria parasite actin filaments are very short. *J Mol Biol* **349:** 113–125.

Schmitz, S., Schaap, I.A.T., Kleinjung, J., Harder, S., Grainger, M., Calder, L., *et al.* (2010) Malaria parasite actin polymerization and filament structure. *J Biol Chem* **285:** 36577–36585.

Schüler, H., and Matuschewski, K. (2006) Regulation of apicomplexan microfilament dynamics by a minimal set of actin-binding proteins. *Traffic* **7:** 1433–1439.

Schüler, H., and Peti, W. (2007) Structure-function analysis of the filamentous actin binding domain of the neuronal scaffolding protein spinophilin. *FEBS J* **275:** 59–68.

Schüler, H., Mueller, A.-K., and Matuschewski, K. (2005) Unusual properties of *Plasmodium falciparum* actin: new insights into microfilament dynamics of apicomplexan parasites. *FEBS Lett* **579:** 655–660.

Sibley, L.D. (2011) Invasion and intracellular survival by protozoan parasites. *Immunol Rev* **240:** 72–91.

Siden-Kiamos, I., Ganter, M., Kunze, A., Hliscs, M., Steinbüchel, M., Mendoza, J., *et al.* (2011) Stage-specific depletion of myosin A supports an essential role in motility of malarial ookinetes. *Cell Microbiol* **13:** 1996–2006.

Siden-Kiamos, I., Louis, C., and Matuschewski, K. (2012) Evidence for filamentous actin in ookinetes of a malarial parasite. *Mol Biochem Parasitol* **181:** 186–189.

Sinden, R.E., Dawes, E.J., Alavi, Y., Waldock, J., Finney, O., Mendoza, J., *et al.* (2007) Progression of *Plasmodium berghei* through *Anopheles stephensi* is density-dependent. *PLoS Pathog* **3:** e195.

Sinnar, S.A., Antoku, S., Saffin, J.-M., Cooper, J.A., and Halpain, S. (2014) Capping protein is essential for cell migration in vivo and for filopodial morphology and dynamics. *Mol Biol Cell* **25:** 2152–2160.

Skillman, K.M., Diraviyam, K., Khan, A., Tang, K., Sept, D., and Sibley, L.D. (2011) Evolutionarily divergent, unstable filamentous actin is essential for gliding motility in apicomplexan parasites. *PLoS Pathog* **7:** e1002280.

Skillman, K.M., Ma, C.I., Fremont, D.H., Diraviyam, K., Cooper, J.A., Sept, D., and Sibley, L.D. (2013) The unusual dynamics of parasite actin result from isodesmic polymerization. *Nat Commun* **4:** 2285.

Soeno, Y., Abe, H., Kimura, S., Maruyama, K., and Obinata, T. (1998) Generation of functional beta-actinin (CapZ) in an *E. coli* expression system. *J Muscle Res Cell Motil* **19:** 639–646.

Sun, H.Q., Wooten, D.C., Janmey, P.A., and Yin, H.L. (1994) The actin side-binding domain of gelsolin also caps actin filaments. Implications for actin filament severing. *J Biol Chem* **269:** 9473–9479.

Takeda, S., Minakata, S., Koike, R., Kawahata, I., Narita, A., Kitazawa, M., *et al.* (2010) Two distinct mechanisms for actin capping protein regulation – steric and allosteric inhibition. *PLoS Biol* **8:** e1000416.

Vanderberg, J.P. (1974) Studies on the motility of *Plasmodium* sporozoites. *J Protozool* **21:** 527–537.

Wear, M.A., and Cooper, J.A. (2004) Capping protein: new insights into mechanism and regulation. *Trends Biochem Sci* **29:** 418–428.

Wear, M.A., Yamashita, A., Kim, K., Maéda, Y., and Cooper, J.A. (2003) How capping protein binds the barbed end of the actin filament. *Curr Biol* **13:** 1531–1537.

Weiss, V.H., McBride, A.E., Soriano, M.A., Filman, D.J., Silver, P.A., and Hogle, J.M. (2000) The structure and oligomerization of the yeast arginine methyltransferase, Hmt1. *Nat Struct Biol* **7:** 1165–1171.

Wong, W., Skau, C.T., Marapana, D.S., Hanssen, E., Taylor, N.L., Riglar, D.T., *et al.* (2011) Minimal requirements for actin filament disassembly revealed by structural analysis of malaria parasite actin-depolymerizing factor 1. *Proc Natl Acad Sci USA* **108:** 9869–9874.

Xu, J., Casella, J.F., and Pollard, T.D. (1999) Effect of capping protein, CapZ, on the length of actin filaments and mechanical properties of actin filament networks. *Cell Motil Cytoskeleton* **42:** 73–81.

Yamashita, A., Maeda, K., and Maéda, Y. (2003) Crystal structure of CapZ: structural basis for actin filament barbed end capping. *EMBO J* **22:** 1529–1538.

Supporting information

Additional supporting information may be found in the online version of this article at the publisher's web-site.